Brief communication: Impacts of ocean-wave-induced breakup of Antarctic sea ice via thermodynamics in a standalone version of the CICE sea-ice model

Luke G. Bennetts[1], Siobhan O'Farrell[2], and Petteri Uotila[3]

[1]School of Mathematical Sciences, University of Adelaide, Adelaide, SA, Australia
[2]CSIRO Ocean and Atmosphere, Aspendale, VIC, Australia
[3]Finnish Meteorological Institute, Helsinki, Finland

Correspondence to: L. G. Bennetts (luke.bennetts@adelaide.edu.au)

Abstract. Impacts of wave-induced breakup of Antarctic sea ice on ice concentration and volume are investigated using a modified version of the CICE sea ice model, run in standalone mode from 1979–2010. ~~Model outputs show that breakup reduces ice concentration by up to 0.3–0.4 in a vicinity of the ice edge during the summer, and total ice volume by over 500 km^3.~~ Model outputs show that during summer wave-induced breakup reduces local ice concentration by up to 0.3–0.4 in a vicinity of the ice edge, and total ice volume by up to a factor of 0.1–0.2.

1 Introduction

Speculation surrounding the impacts of ocean surface waves on the world's sea ice is building. In the Antarctic, the speculation has been fuelled by Kohout et al. (2014)'s findings that trends in ice-edge contraction (from satellite observations) are closely correlated to trends in increasing local significant wave heights (from a numerical model) and, conversely, trends in ice-edge expansion are correlated to trends in decreasing significant wave heights. They attributed these correlations to large-amplitude storm waves propagating into the ice-covered ocean and breaking up the ice cover into relatively small floes, which are more mobile and vulnerable to melting. This relationship can be inferred from descriptions of the way in which waves regulate the morphology of the ice cover in the first 10s to 100s of kilometres in from the ice edge, originally made by Squire, Wadhams and co-workers in the 1970s (see, e.g., the review by Squire et al., 1995) — a region often referred to as the marginal ice zone, although the term is not adopted in this study due to ambiguity in its definition. Kohout et al. (2014) suggested that incorporating wave impacts on sea ice into climate models will empower the models to capture sea ice responses to climate change, for example, the regional variability of trends in Antarctic sea-ice extent (Stammerjohn et al., 2008).

This study constitutes the first quantification of Antarctic sea-ice breakup by waves on ice concentration and volume. It uses a standalone version of the CICE sea-ice model, modified to include wave-induced breakup, with wave forcing provided by a Wavewatch III wave-model hindcast in ice-free grid cells close to the ice edge. Wave energy advects into cells containing ice cover, where models of wave-energy attenuation due to ice cover and wave-induced ice breakup are applied, in a similar manner to the operational ice/ocean model wave–ice interaction component developed by Williams et al. (2013a, b).

CICE v4.1 (Hunke and Lipscomb, 2010) is used for the study, in which floe diameters appear in the lateral ice-melt model only, and are set to be 300 m throughout the ice cover by default. Breakup reduces mean floe diameters typically to 20–100 m in cells extending ∼100 km in from the ice edge, beyond which the wave energy is no longer strong enough to break the ice. When ocean temperatures are high enough to melt ice, the reduced diameters promote lateral melt, reducing the ice concentration, which, in turn, reduces the ice strength, so that breakup indirectly impacts both ice concentration and volume through dynamic processes. Model outputs show that during the summer wave-induced breakup reduces local ice concentration by up to 0.3–0.4 and total ice volume by ~~> 500 km³~~ up to a factor of 0.1–0.2. During the winter, the ice concentration recovers, but volume changes persist, becoming dispersed over the inner ice pack.

2 Model

CICE uses an ice-thickness-distribution function $g(\mathbf{x}_{ij}, t : h)$ to describe the sea-ice cover, in which $\mathbf{x}_{ij}$ denotes a grid cell on the ocean surface, indexed i in longitude and j in latitude, t denotes time, and h denotes ice thickness, with $g(\mathbf{x}_{ij}, t : h)dh$ the fractional area of ice in cell-ij with thickness in the interval $(h, h + dh)$. The ice-thickness distribution is calculated as a numerical approximation of the ice-thickness-evolution equation (Thorndike et al., 1975)

$$\frac{\partial g}{\partial t} = -\nabla \cdot (g\mathbf{u}) - \frac{\partial}{\partial h}(fg) + \psi, \tag{1}$$

using discrete time steps with a nominal global time step ~~length of one hour~~ $\Delta t = 1$ h, a horizontal tripolar grid with a nominal resolution of one latitudinal/longitudinal degree, and partitioning of the ice into discrete thickness categories (five categories plus open water are used for this study, as standard). The first term on the right-hand side of Eqn. (1) denotes ice advection, where $\mathbf{u}$ is ice velocity, calculated via the elastic–viscous–plastic (EVP) rheology model of Hunke and Dukowicz (1997). The second term denotes thermodynamic thickness redistribution, where f is the rate of melting or freezing. The final term denotes mechanical redistribution due to ridging.

Waves are introduced into the model using the wave-energy-density spectrum, $S(\mathbf{x}_{ij}, t : \omega, \theta)$, where ω and θ denote angular frequency and wave direction, respectively. This is the standard description of waves in oceanic general-circulation models. At the beginning of each time step, incident spectra are prescribed in grid cells at a latitude outside the ice cover but as close to the ice cover as possible. For expediency, in each cell at the incident latitude, the wave field is set to be a Bretschneider spectrum, defined by a significant wave height and a peak period, propagating in the mean wave direction. In subsequent cells, directions are calculated as averages of the wave directions entering the respective cells, weighted according to the associated wave energy.

Assuming steady-state conditions over a time step, the spatial distribution of wave energy in the ice-covered ocean is calculated according to a discrete version of the wave-energy-balance equation

$$(\cos\theta, \sin\theta) \cdot \nabla S = -\alpha S. \tag{2}$$

The attenuation coefficient, $\alpha(\mathbf{x}_{ij}, t:\omega)$, is set as

$$\alpha = \alpha_0 \equiv c(\beta_2\hat{\alpha}_2\omega^2 + \beta_4\hat{\alpha}_4\omega^4), \quad \text{where the coefficients} \quad \beta_2\hat{\alpha}_2 \approx 7.68\times10^{-5} \quad \text{and} \quad \beta_4 = \hat{\alpha}_4 \approx 4.21\times10^{-5} \tag{3}$$

(units of time$^2\times$distance^{-1} and time$^4\times$distance^{-1}, respectively), based on Meylan et al. (2014)'s empirical model, scaled according to the areal concentration of sea ice on the ocean surface, $c(\mathbf{x}_{ij}, t)$.

In each cell, the floe-size distribution is defined by a representative floe diameter $D(\mathbf{x}_{ij})$, for consistency with the assumptions underlying the lateral-melt model, described below. At the beginning of a simulation, the diameters are set to the relatively large value $D(\mathbf{x}_{ij}) = D_{\text{mx}} = 300\,\text{m}$, for consistency with the value used throughout the ice cover in existing versions of CICE. For cells in which wave energy is non-negligible, Williams et al. (2013a)'s ice-breakup criterion is applied, with the diameter of the broken floes denoted $D_{\text{bk}} < D_{\text{mx}}$. ~~Following Bennetts et al. (2015), the representative floe diameter in cell-ij post wave-induced breakup is calculated as a weighted average of the broken-floe diameter over the fraction of the cell where the waves are strong enough to cause breakup, a_{bk}, and the diameter in the cell at the beginning of the time step, D_0, in the remaining fraction, i.e. $D(\mathbf{x}_{ij}) = a_{\text{bk}}(\mathbf{x}_{ij})D_{\text{bk}}(\mathbf{x}_{ij}) + (1 - a_{\text{bk}}(\mathbf{x}_{ij}))D_0(\mathbf{x}_{ij})$.~~ Following wave-induced breakup, the representative floe diameter in cell-ij is calculated as the weighted average

$$D(\mathbf{x}_{ij}) = a_{\text{bk}}(\mathbf{x}_{ij})D_{\text{bk}}(\mathbf{x}_{ij}) + (1 - a_{\text{bk}}(\mathbf{x}_{ij}))D_0(\mathbf{x}_{ij}), \tag{4}$$

where D_0 is the representative diameter in the cell at the beginning of the time step, and $a_{\text{bk}} = L_{\text{bk}}/L_{\text{cl}}$, in which L_{cl} is the length of the cell in the southwards direction, and L_{bk} is the distance the wave spectrum propagates southwards through the cell, whilst being attenuated according to Eqn. (2), and maintains sufficient energy to cause breakup (Bennetts et al., 2015). For cells at the outermost fringes of the ice-covered ocean, where the ice is too thin and compliant to be broken by waves, the floes diameters are assumed to be small, and assigned the representative diameter $D = D_{\text{mn}}$.

In cells where breakup occurs, the ~~broken-floe~~ representative diameter of broken floes, D_{bk}, is calculated by assuming the in-cell floe-size distribution obeys a split power law, as observed by Toyota et al. (2011) (noting that alternative distributions have been postulated for the transition from small–large floes, e.g. Herman, 2010). ~~and with Williams et al. (2012)'s~~ The probability-density function for the split power law, $p(d)$, where d denotes floe diameter, is defined by

$$p(d) = \frac{\mathbb{P}_0\beta_0\gamma_0}{d^{\gamma_0+1}} \quad \text{if} \quad d \in [D_{\text{mn}}, D_{\text{cr}}), \quad \text{where} \quad \beta_0 = \left(D_{\text{mn}}^{-\gamma_0} - D_{\text{cr}}^{-\gamma_0}\right)^{-1}, \tag{5a}$$

$$p(d) = \frac{(1-\mathbb{P}_0)\beta_1\gamma_1}{d^{\gamma_1+1}} \quad \text{if} \quad d \in [D_{\text{cr}}, \infty), \quad \text{where} \quad \beta_1 = D_{\text{cr}}^{\gamma_1}, \tag{5b}$$

and $p(d) = 0$ if $d < D_{\text{mn}}$ (Williams et al., 2012). Here, D_{mn} represents a minimum floe diameter, which is chosen to be equal to the small-floe diameter; ~~for small floes for simplicity;~~ D_{cr} is a critical diameter marking the transition from small to large floes (found to be in the range 15–40 m by Toyota et al., 2011), and $\gamma_{10} = 1.15$ and $\gamma_{21} = 2.5$ are representative exponents for small- and large-floe regimes, respectively (Toyota et al., 2011). The quantity $\mathbb{P}_0 \in [0,1]$ weights the distribution towards small floes (large $\mathbb{P}_0$) or large floes (small $\mathbb{P}_0$). Its value is set as

$$\mathbb{P}_0 = 1 - q\left(\frac{D_{\text{pr}}}{D_{\text{cr}}}\right)^{\gamma_1} \qquad \text{where} \qquad D_{\text{pr}} = \lambda/2 \qquad \text{is the predicted breakup diameter,} \tag{6}$$

equal to the distance between successive strain maxima for a regular wave train at the dominant wavelength λ for the spectrum S, propagating through an infinitely long, uniform floe (Williams et al., 2013a; Bennetts et al., 2015), so that a chosen proportion q of floe diameters are greater than D_{pr}. In the uncommon event that $D_{\text{pr}} < D_{\text{cr}}$ then $\mathbb{P}_0 = 0$, noting that D_{cr} approximates the theoretical diameter below which flexural breakup cannot occur (Toyota et al., 2011). The broken-floe diameter D_{bk} is the mean diameter ~~in a given cell, i.e.~~

$$D_{\text{bk}} = \int_{D_{\text{mn}}}^{\infty} p(d)d\,\mathrm{d}d\,\underline{pD\,\mathrm{d}D} = \frac{\mathbb{P}_0\gamma_0\beta_0(D_{\text{mn}}^{1-\gamma_0} - D_{\text{cr}}^{1-\gamma_0})}{\gamma_0 - 1} + \frac{(1-\mathbb{P}_0)\gamma_1\beta_1 D_{\text{cr}}^{1-\gamma_1}}{\gamma_1 - 1}. \tag{7}$$

The breakup model is applied at the beginning of each CICE time-step, allowing the reduced floe diameters to affect other CICE-model components. The reduced diameters directly affect the ~~contribution of lateral melting~~ fraction of ice that melts laterally, r_{lat}, ~~to reducing the ice concentration~~ via the discrete version of Steele (1992)'s model

$$r_{\text{lat}} = \frac{\pi \Delta t w_{\text{lat}}}{\mu D}, \tag{8}$$

which assumes floes in a given cell are identical. Here $\mu = 0.66$ is a geometric parameter, and $w_{\text{lat}} = 1.6\Delta T^2 \times 10^{-6}$ (units of distance$\times$time^{-1}) is the rate of lateral melt, in which ΔT is the temperature difference of the sea surface above that of the bottom of the ice (set to zero if the difference is negative). The diameter is updated at the end of the thermodynamic routine to account for lateral melt. ~~The floe-diameter parameter is a tracer field in CICE, and is transported within each ice category to give the total floe-size distribution at the end of a time step.~~

During the summer months, when the ice is weaker and towards its minimum extent, waves cause breakup close to the coastline. The existing thermodynamic models in CICE do not increase the diameters of these broken floes fast enough through the winter to create a realistic seasonal cycle for the floe-diameter distribution. Therefore, an ad-hoc floe-bonding scheme is applied, in which the floe diameter in a given cell is doubled if the freezing potential in that cell is positive, up to the maximum diameter D_{mx}.

The representative diameter, D, is transported by: (i) setting the floe diameter to be identical for each of the different thickness categories, and transporting the floe diameter as an area tracer for the different thickness categories; and (ii) setting the new representative diameters to be the diameters of the thinnest ice category (cat. 1). Step (ii) is a non-physical simplifying assumption; tests indicate that this assumption does not affect the concentration changes due to breakup presented in § 3.

3 Results

The model was run from 1979–2010 using input wave data generated by a Wavewatch III model hindcast (Durrant et al., 2013), and atmospheric and oceanic data from the U.S. National Center for Environmental Prediction's Climate Forecast System Reanalysis (NCEP's CFSR, Saha et al., 2010). The minimum and critical floe diameters are set as $D_{\text{mn}} = 5$ m and $D_{\text{cr}} = 30$ m, and, following breakup, the proportion $q = 0.05$ of floe diameters are set to be greater than the predicted breakup diameter D_{pr}.

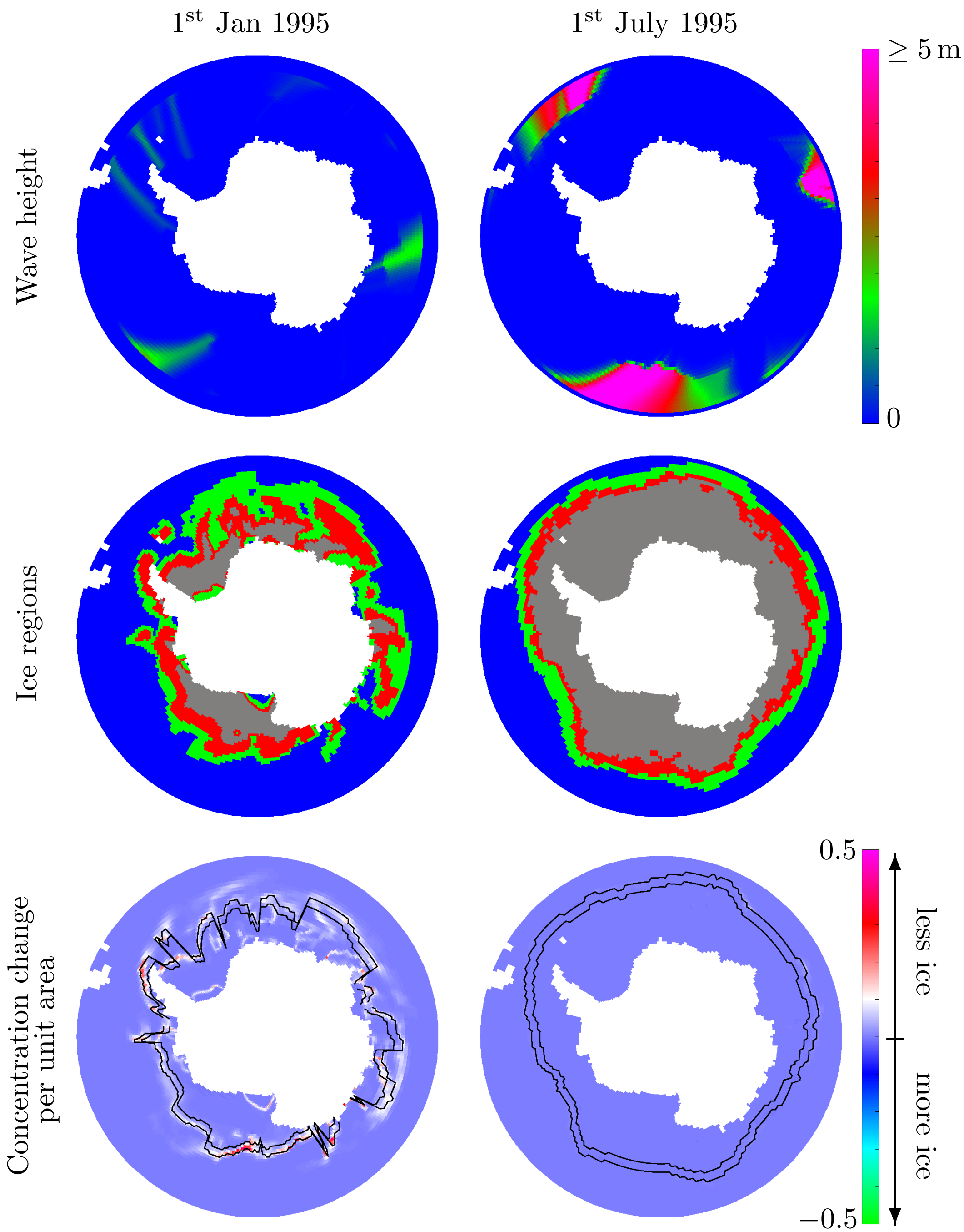

Figure 1. Example model outputs using minimum and critical floe diameters $D_{\mathrm{mn}} = 5\,\mathrm{m}$ and $D_{\mathrm{cr}} = 30\,\mathrm{m}$, and $q = 0.05$. The ~~left-hand column~~ top row shows the significant wave heights. The middle ~~column~~ row shows the ice regions: small floes (green), wave-broken floes (red), unbroken floes (grey) and no ice/open water (blue). The ~~right-hand column~~ bottom row shows the change in concentration between the simulations without and with breakup. The ~~top row~~ left-hand column is representative of results in austral summer, and the ~~bottom row~~ right-hand panel of winter.

Fig. 1 shows example model outputs for two dates during 1995 (i.e. a year half-way through the simulation), representative of results in summer (1st January, left-hand panels~~ in top row~~) and winter (1st July, ~~bottom~~ right). The panels in the ~~left-hand column~~ top row show significant wave heights, with the sharp outer boundaries of non-zero wave heights indicating the latitudes at which data is extracted from the wave model. This boundary is farther north in the winter because the ice extent is greater than in the summer. The regions of rapid wave-height decrease with respect to southward distance indicate attenuation of wave energy due to ice cover. In the summer, packets of wave energy are able to propagate almost to the coastline, particularly around the Antarctic peninsula, due to reduced ice cover in that locality.

The middle ~~column~~ row shows the extent of ice coverage, with the ice divided into regions according to floe size. Regions of small diameter floes (green) are identified as those cells for which $D \leq D_{\rm mn} = 5\,$m, wave-broken floes (red) are the floe-size interval $D_{\rm mn} < D \leq 250\,$m, and unbroken floes (grey) are $D > 250\,$m. The ~~right-hand column~~ bottom row shows the impact of the small and broken floes on ice concentration, in terms of the difference in concentration between the simulation without breakup ($D = 300\,$m) and the simulation with breakup, with positive values indicating decreases in concentration due to breakup.

The Southern Ocean experiences the strongest waves during winter, as indicated in the ~~left-hand column~~ top row. However, the areas covered by regions of broken ice are comparable between the two seasons (approximately 10 % smaller in the summer for the dates shown in the middle row), as the lower summer ice concentration allows waves to penetrate deeper into the ice-covered ocean, relative to their incident energy. The ice is structured into approximately uniform bands in the winter, whereas in the summer coastal effects complicate the structure.

In the summer, the broken ice decreases the ice concentration in a vicinity of the ice edge, with reductions of ~ 0.1 common, but numerous pockets of 0.3–0.4 reductions apparent. The region most impacted by breakup is estimated by the region bounded by the two black lines, where the outer black line denotes the first cell (with respect to each longitude) at which the ice concentration exceeds 0.1, and the inner black line represents three cells ~~further~~ farther in (or land if that begins before the third cell). During the winter, the concentration change is too small to be visible on the scale shown (order 0.01), as the temperatures are too low to melt the broken floes.

Fig. 2 shows mean–monthly ice concentrations at the ice edge (the region bounded by the black lines in the ~~right-hand column~~ bottom row of Fig. 1), for each simulation year. Results are again shown for January and July, as representations of summer and winter conditions, respectively. Data were generated ~~for~~ by simulations without breakup ($\times$) and with breakup (•). For the summer conditions, additional data indicate sensitivities of concentration changes to: (i) the floe-size parameters, with data given for simulations in which $D_{\rm mn}$, $D_{\rm cr}$ and q are decreased to $D_{\rm mn} = 2.5\,$m, $D_{\rm cr} = 20\,$m, and $q = 0.025$ (▼) and increased to $D_{\rm mn} = 10\,$m, $D_{\rm cr} = 40\,$m and $q = 0.1$ (▲); and (ii) increasing or decreasing the wave-attenuation coefficient, α, by an order of magnitude ($\alpha = 10\alpha_0$, ▲, and $\alpha = \alpha_0/10$, ▼, respectively). The ranges of floe sizes and attenuation rates are within the limits of present uncertainty.

As indicated by Fig. 2 and the bottom–left panel of Fig. 1, breakup has negligible impact on ice concentration during winter. During the summer, breakup reduces the concentration, with the mean decrease being ~ 0.08 for the parameters used in Fig. 1 (neglecting the first, spin-up year of the simulation). Reducing the floe-size parameters increases the impact of breakup (as

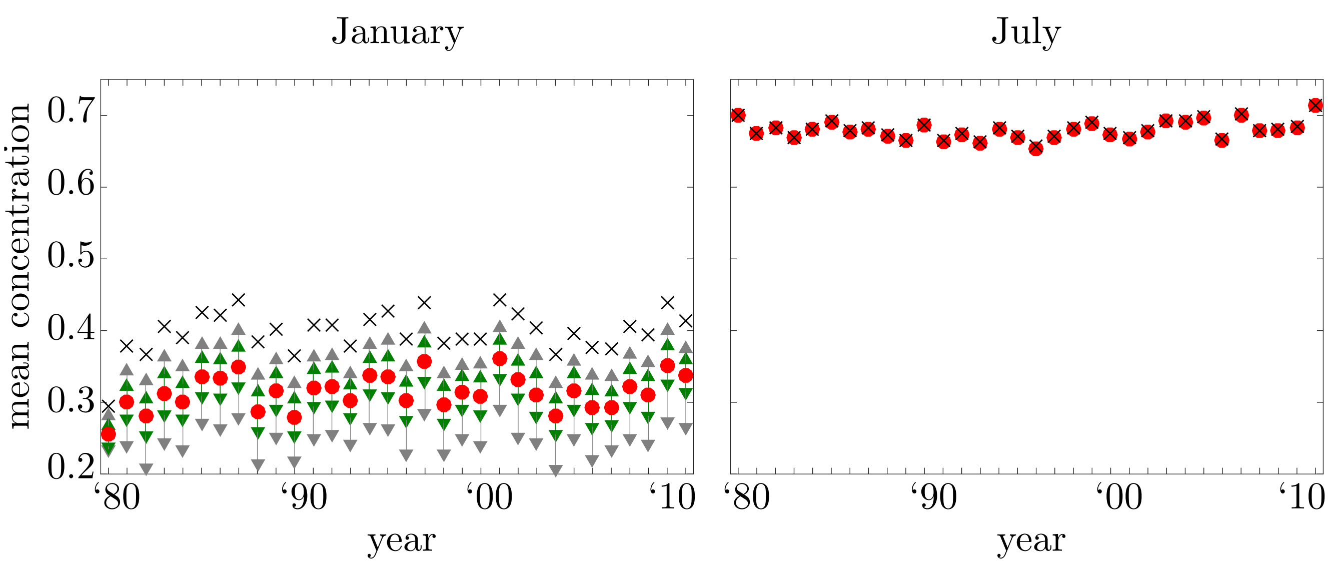

Figure 2. The mean–monthly ice concentration at the ice edge (the region bounded by the black lines in the bottom row of Fig. 1), for January (left-hand panel) and July (right). Results are for the simulation without breakup ($\times$) and with breakup for: the parameters considered in Fig. 1 ($D_{\mathrm{mn}} = 5$ m, $D_{\mathrm{cr}} = 30$ m, and $q = 0.05$, ●); smaller floes $D_{\mathrm{mn}} = 2.5$ m, $D_{\mathrm{cr}} = 20$ m and $q = 0.025$ (▼); larger floes $D_{\mathrm{mn}} = 10$ m, $D_{\mathrm{cr}} = 40$ m and $q = 0.1$ (▲); a decreased attenuation rate $\alpha = \alpha_0/10$ ~~an increased attenuation rate $\alpha = 10\alpha_0$~~ (▼); and an increased attenuation rate $\alpha = 10\alpha_0$ ~~a decreased attenuation rate $\alpha = \alpha_0/10$~~ (▲).

smaller floes melt more rapidly than larger ones), and increasing them reduces the impact, with the mean reductions compared to the simulation without breakup being ~ 0.11 and 0.06, respectively. Similarly, reducing the attenuation rate increases the impact (as the waves maintain their strength for greater distances into the ice-covered ocean), and increasing the attenuation rate has the opposite effect — the mean reductions are ~ 0.15 and 0.04, respectively.

The top panels of Fig. 3 show changes in ice volume per unit area due to breakup, for the two dates used in Fig. 1, i.e. results representative of summer (1st January 1995, left-hand panel) and winter (1st July 1995, right). During the summer, breakup decreases the ice volume, particularly at the ice edge, where losses of ~ 0.5 m per unit area are common. ~~with losses of up to $\sim 2.7\,\mathrm{km}^3$ in individual cells~~ The pattern of the decreases is strongly correlated with the concentration decreases shown in the top–right panel of Fig. 1. ~~However, reductions in ice thickness forced by dynamic processes also contribute to volume losses with mean in-cell thicknesses up to 0.96 m thinner with breakup for the date shown.~~ During the winter, ~~volume losses of $\sim 0.5\,\mathrm{km}^3$ per grid cell (but up to $1\,\mathrm{km}^3$)~~ regions of volume loss 0.1–0.3 m per unit area are visible in the interior of the ice cover (the unbroken ice region). This contrasts with the negligible concentration losses on the same date shown in ~~bottom–left~~ the bottom–right panel of Fig. 1. The volume losses result from summer thickness reductions forced by dynamic processes being restored at a slower rate than concentration. Ice advection disperses the losses over large regions.

The bottom–left panel of Fig. 3 shows ~~mean–monthly decreases in ice volumes~~ volume decreases due to breakup as proportions of the total ice cover without breakup, over a typical six-year interval. The ice volumes are sums over the total ice cover (for cells with concentrations greater than 0.1, ♦) and cells at the ice edge (the region between the black lines, $*$). Seasonal cycles are evident, with, for example, peaks in both proportions occurring in March; the peaks for the full cover are between 0.13–0.20, and the peaks at the ice edge are between 0.09–0.14. ~~maximum total volume losses of 600–760 km^3 occurring in December and minimum losses of 260–320 km^3 occurring in August. Losses at the ice edge are negligible during winter, but are up to 470 km^3 during summer, accounting for increases in total volume loss during that season.~~ During June and July, losses at the ice edge due to wave-induced breakup contribute typically less than 5% of the total volume losses only, whereas, during November–March a large proportion (54–68%) of the overall losses occur at the ice edge, as indicated in the top–left panel of Fig. 3.

The bottom–right panels of Fig. 3 show decreases in total ice volume per degree latitude on 1st January (bottom panel) and 1st July (top), over the full 32 years of the simulations, in terms of the median values, and the spread, in terms of the 25th and 75th percentiles. Data are split into losses in the eastern (—) and western (—) sectors of Antarctica (as shown in the top panels of Fig. 3). During the summer, when the increased lateral melt of the reduced floe diameters impacts ice concentration, volume ~~the~~ losses in the two sectors are similar. ~~During the winter, western-sector losses outweigh those of the eastern sector, with median losses for the western sector on average 0.57 km^3 greater than the eastern sector. This is attributed to a significant proportion of the East Antarctic sea ice, which that is impacted by breakup during the summer, melting during February, so that the winter ice is largely composed of new ice, with no memory of the breakup.~~ However, only the western sector carries the bulk of its volume loss into winter, as a significant proportion of East Antarctic sea ice affected by breakup during early–mid summer melts during February, so that the winter ice is largely composed of new ice.

4 Discussion

The findings of this pilot study indicate that increased lateral ice melt over the first ~ 100 km in from the ice edge, due to small wave-broken floes, and the follow-on effects on ice dynamics, impact ice concentration and volume in a vicinity of the edge during winter, and ice volume in the interior pack throughout the year. Horvat et al. (2016)'s coupled ice–ocean–atmosphere model, which includes interactions between floe diameters, ocean circulation and ice melt, indicates that lateral melt remains important for sea-ice evolution for floe diameters orders of magnitude larger than the O(30 m) limit given by Steele (1992)'s model, as used in CICE. Presumably, therefore, integrating diameter–circulation–melt interactions into the modified version of CICE would strengthen the impacts of breakup. Moreover, integrating Feltham (2005)'s granular floe-size dependent rheology would provide a direct impact of breakup on ice dynamics. Applying the modified CICE model in a fully-coupled setting will unlock feedbacks triggered by the breakup — for example, the reduced concentration due to increased lateral melt releasing more oceanic heat to the atmosphere, thus increasing upwelling of ocean heat through convection and hence promoting further ice melt — permitting studies into influences on long-term trends in ice concentration, volume and also extent. ~~If the community judges~~ If further research finds the impacts of floe-size dependent processes to be significant, future large-scale sea-ice models may be developed along the lines of the theories for coupled ice-thickness and floe-size evolution outlined by Zhang et al. (2015) and Horvat and Tziperman (2015).

5 Code availability

The Australian Antarctic Data Centre hosts the code used for this study at doi:10.4225/15/57D0EA42ED985.

Acknowledgements. The authors thank Mark Hemer for providing advice on the wave data used. The Australian Research Council (DE130101571) and the Australian Antarctic Science Program (Project 4123) funded this investigation. The Academy of Finland supports PU (Contract 264358).

References

Bennetts, L. G., O'Farrell, S., Uotila, P., and Squire, V. A.: An idealised wave–ice interaction model without subgrid spatial or temporal discretisations, Ann. Glaciol., 56, 258–262, 2015.

Durrant, T., Hemer, M., Trenham, C., and Greenslade, D.: CAWCR Wave Hindcast 1979-2010. v7, Tech. rep., CSIRO. Data Collection, doi:http://doi.org/10.4225/08/523168703DCC5, 2013.

Feltham, D. L.: Granular flow in the marginal ice zone, Phil. Trans. R. Soc. Lond. A, 363, 1677–1700, doi:10.1098/rsta.2005.1601, 2005.

Herman, A.: Sea-ice floe-size distribution in the context of spontaneous scaling emergence in stochastic systems, Phys. Rev. E, 81, 066 123, doi:10.1103/PhysRevE.81.066123, 2010.

Horvat, C. and Tziperman, E.: A prognostic model of the sea ice floe size and thickness distribution, Cryophere, 9, 2119–2134, doi:10.5194/tcd-9-2955-2015, 2015.

Horvat, C., Tziperman, E., and Campin, J.-M.: Interaction of sea ice floe size, ocean eddies, and sea ice melting, Geophys. Res. Lett., 43, 8083–8090, doi:10.1002/2016GL069742, 2016.

Hunke, E. C. and Dukowicz, J. K.: An elastic-viscous-plastic model for sea ice dynamics, J. Phys. Oceangr., 27, 1849–1867, 1997.

Hunke, E. C. and Lipscomb, W. H.: CICE : the Los Alamos Sea Ice Model Documentation and Software User's Manual Version 4.1 (LA-CC-06-012), Tech. rep., T-3 Fluid Dynamics Group, Los Alamos National Laboratory, 2010.

Kohout, A. L., Williams, M. J. M., Dean, S. M., and Meylan, M. H.: Storm-induced sea-ice breakup and the implications for ice extent., Nature, 509, 604–7, doi:10.1038/nature13262, 2014.

Meylan, M. H., Bennetts, L. G., and Kohout, A. L.: In-situ measurements and analysis of ocean waves in the Antarctic marginal ice zone, Geophys. Res. Lett., 41, 5046–5051, 2014.

Saha, S., Moorthi, S., Pan, H.-L., Wu, X., Wang, J., Nadiga, S., Tripp, P., Kistler, R., Woollen, J., Behringer, D., Liu, H., Stokes, D., Grumbine, R., Gayno, G., Wang, J., Hou, Y.-T., Chuang, H.-Y., Juang, H.-M. H., Sela, J., Iredell, M., Treadon, R., Kleist, D., Van Delst, P., Keyser, D., Derber, J., Ek, M., Meng, J., Wei, H., Yang, R., Lord, S., van den Dool, H., Kumar, A., Wang, W., Long, C., Chelliah, M., Xue, Y., Huang, B., Schemm, J.-K., Ebisuzaki, W., Lin, R., Xie, P., Chen, M., Zhou, S., Higgins, W., Zou, C.-Z., Liu, Q., Chen, Y., Han, Y., Cucurull, L., Reynolds, R. W., Rutledge, G., and Goldberg, M.: NCEP Climate Forecast System Reanalysis (CFSR) 6-hourly Products, January 1979 to December 2010, http://dx.doi.org/10.5065/D69K487J, 2010.

Squire, V. A., Dugan, J. P., Wadhams, P., Rotter, P. J., and Liu, A. K.: Of ocean waves and sea ice, Annu. Rev. Fluid Mech., 27, 115–168, 1995.

Stammerjohn, S., Martinson, D. G., Smith, R. C., Yuan, X., and D., R.: Trends in Antarctic sea ice retreat and advance and their relation to El Nino–Southern Oscillation and southern annular mode variability, J. Geophys. Res., 113, C03S90, 2008.

Steele, M.: Sea ice melting and floe geometry in a simple ice-ocean model, J. Geophys. Res., 94, 17,729–17,738, 1992.

Thorndike, A. S., Rothrock, D. A., Maykut, G. A., and Colony, R.: The Thickness Distribution of Sea Ice, J. Geophys. Res., 80, 4501, doi:10.1029/JC080i033p04501, 1975.

Toyota, T., Haas, C., and Tamura, T.: Size distribution and shape properties of relatively small sea-ice floes in the Antarctic marginal ice zone in late winter, Deep Sea Res. Pt. II, 58, 1182–1193, doi:10.1016/j.dsr2.2010.10.034, 2011.

Williams, T. D., Bennetts, L. G., Squire, V. A., Dumont, D., and Bertino, L.: Towards the inclusion of wave–ice interactions in large-scale models for the Marginal Ice Zone, ArXiV, 2012.

Williams, T. D., Bennetts, L. G., Dumont, D., Squire, V. A., and Bertino, L.: Wave–ice interactions in the marginal ice zone. Part 1: Theoretical foundations, Ocean Model., 71, DOI: 10.1016/j.ocemod.2013.05.010, 2013a.

Williams, T. D., Bennetts, L. G., Dumont, D., Squire, V. A., and Bertino, L.: Wave–ice interactions in the marginal ice zone. Part 2: Numerical implementation and sensitivity studies along 1D transects of the ocean surface, Ocean Model., 71, DOI: 10.1016/j.ocemod.2013.05.011, 2013b.

Zhang, J., Schweiger, A., Steele, M., and Stern, H.: Sea ice floe size distribution in the marginal ice zone: Theory and numerical experiments, J. Geophys. Res., 120, 3484–3498, 2015.

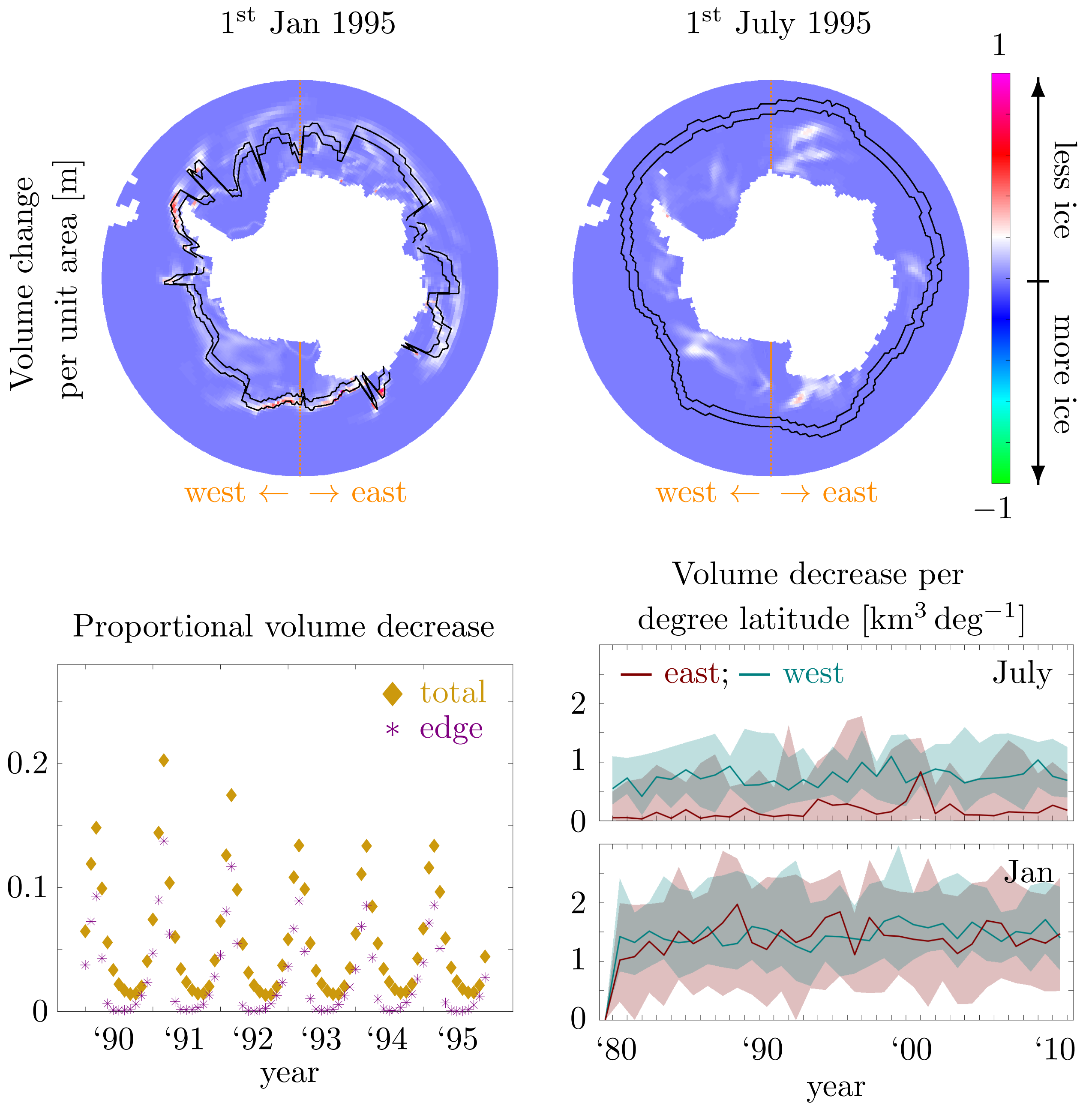

Figure 3. Top row: Snapshots of ice volume changes per unit area between simulations without and with breakup ($D_0 = 5$ m, $D_{cr} = 30$ m and $q = 0.05$). Bottom–left panel: ~~Mean–monthly decreases in ice volume,~~ Proportional volume decrease on first day of month over total ice cover (◆) and at ice edge ($*$), for 1990–1995. Bottom–right panels: Median decrease in ice volume per degree latitude for the eastern sector (—) and the western sector (—), on 1st January (bottom panel) and 1st July (top) for all simulation years. Shaded regions show corresponding 25th to 75th percentile ranges.

Dear Chris

The work shown here is extremely exciting. The inclusion of wave-breaking and a true floe thermodynamics into CICE is an important step towards improving sea ice models, and I look forward to future work implementing this model.

Thanks for your interest in our work and your useful comment.

I wanted to bring up an important, and subtle, issue that I feel should be addressed in this communication and going forward. On pg. 4 line 5, ≪The floe-diameter parameter is a tracer field in CICE, and is transported within each ice category to give the total floe-size distribution at the end of a time step≫. The mean floe diameter, however, does not advect as a tracer.

⋮

Quite possibly the proper mean floe size advection scheme is unimportant, but as you are the first to introduce this type of model, it is unclear, and is exciting to find out. If future models include a fully-evolving FSD, this fix will no longer be necessary.

We consider a "representative" diameter in each cell, as opposed to a mean diameter with respect to a distribution. We set the representative diameter to be the mean diameter of a split PDF if breakup occurs, but without attaching the PDF to the cell, as this would be inconsistent with the Steele model, which considers only a single "average" diameter.

Following the wave–ice routine and lateral melt, we transport the representative diameter by:

(i) Setting the floe diameter to be identical for each thickness category, and transporting the floe diameter as an area tracer for the different categories.

(ii) Setting the new representative diameters to be the diameters of the thinnest ice category (cat. 1).

Step (i) is valid with respect to area normalisiation (a delta function in the FSTD, with respect to floe size). Step (ii) is merely a simplifying assumption; however, it does not impact our results, as shown in the figure below. The figure shows a subset of the data from the left-hand panel of manuscript Fig. 2, comparing the mean–monthly ice concentration at the ice edge during January generated by simulations without breakup (×) and with breakup (•). Additional results are overlaid for the first 12 simulation years, in which part (ii) uses the diameter of cat. 2 ice ($*$) and cat. 3 (□), neglecting thicker ice categories for clarity and on the basis that thinner ice is most prevalent at the ice edge. Cats. 1–3 give virtually indistinguishable results, indicating that "the proper floe size advection scheme is unimportant" – at least for the metrics we focus on in this investigation.

In the revised manuscript, we have expanded the passage on transport of the representative diameter to include the key points of the above discussion.

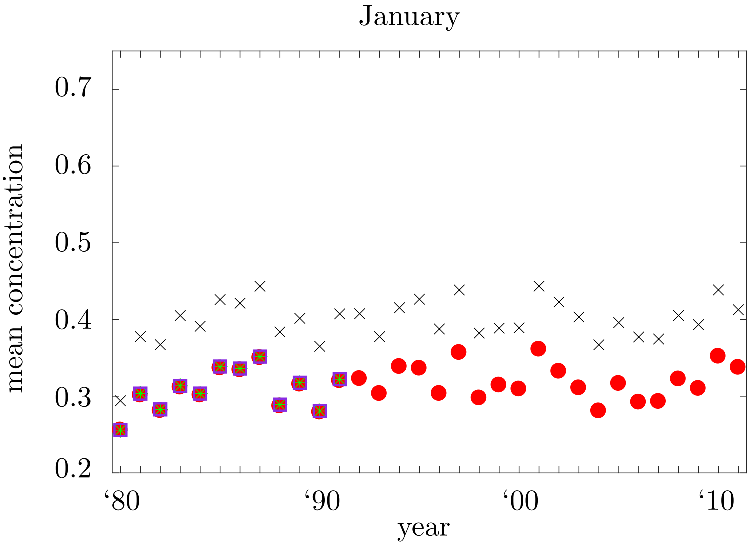

Figure: The left-hand panel of manuscript Fig. 2, excluding data from the smaller/larger floe sizes and attenuation rates, and including results in which the representative floe size following advection is set to the floe size of cat. 2 ice ($*$) and cat. 3 ($\square$), rather than cat. 1.

General comments This paper is clearly written and figures are a clear representation of the results. The paper is a useful pilot study highlighting the potential benefits of inclusion of waves in a sea ice model. More work would be required to make any stronger statements.

Specific comments

1. Does the paper address relevant scientific questions within the scope of TC? Yes, the topic is currently relevant and will interest a significant number of research groups world wide.

2. Does the paper present novel concepts, ideas, tools, or data? Yes, actively including waves within CICE with a focus on Antarctica is novel.

3. Are substantial conclusions reached? This work further highlights the potential for waves to be an important component in CICE in the southern hemisphere. It however does not show that it is. The modelling work would need to be fully coupled and compared against observations to show an improvement over CICE.

4. Are the scientific methods and assumptions valid and clearly outlined? The methods and assumptions are well articulated and appear to be valid.

5. Are the results sufficient to support the interpretations and conclusions? This paper does not overstate the results and highlights that this paper is a pilot study to motivate further research. The results sufficiently show that the modified model, given the assumptions and initial conditions, has the capacity to have an impact on sea ice in summer.

6. Is the description of experiments and calculations sufficiently complete and precise to allow their reproduction by fellow scientists (traceability of results)? The code used in this study is available and the paper is described in such a way that the study should be able to be reproduced.

7. Do the authors give proper credit to related work and clearly indicate their own new/original contribution? The authors give appropriate credit to related work and articulate the new contribution they are making.

8. Does the title clearly reflect the contents of the paper? The title is appropriate.

9. Does the abstract provide a concise and complete summary? yes

10. Is the overall presentation well structured and clear? yes

11. Is the language fluent and precise? yes

12. Are mathematical formulae, symbols, abbreviations, and units correctly defined and used? yes

13. Should any parts of the paper (text, formulae, figures, tables) be clarified, reduced, combined, or eliminated? no

14. Are the number and quality of references appropriate? yes

15. Is the amount and quality of supplementary material appropriate? yes

Technical corrections None spotted

We thank the referee for the supportive review.

We made no changes in response to the comments.

This paper starts with the CICE sea-ice model and adds waves that break up the sea ice in grid cells near the ice edge, causing that ice to melt more quickly in summer due to greater lateral surface area. In general the paper is well conceived and the mechanism is plausible. My comments (below) are minor.

We thank the referee for reviewing our paper, and his/her supportive comments and useful suggestions.

Page 1, Abstract. Total ice volume is reduced by over 500 km^3, but this needs to be put into context. What is the volume of the entire ice cover? Page 2, lines 6-7. Same comment as above.

We now quantify the volume loss in terms of proportion of the total ice volume.

Page 2, equation (3). What are the units of beta_2 and beta_4? From equation (2), alpha must have units of 1/length. The sea-ice concentration, c, is dimensionless, and omega has units of 1/time, so beta_2 must have units of time^2/length, and beta_4 must have units of time^4/length. This should be explicitly noted.

We added units to the values of $\hat{\alpha}_2$ and $\hat{\alpha}_4$ (formerly β_2 and β_4; changed to avoid confusion with β_0 and β_1 used in the FSD).

Page 3, line 10. How is a_bk(x) chosen or determined? There is nothing about it in the rest of the paper.

We now provide a clearer definition of a_{bk}.

Page 3, lines 13-14. The assumption here is that the floe size distribution (FSD) follows a split power law, with one exponent for floes smaller than a critical size and another exponent for floes larger than the critical size, following Toyota et al (2011). This is a dubious formulation of the FSD. First of all, if one actually looks at figure 9 of Toyota et al (2011), one sees that the FSD is a continuously curving concave-down shape, rather than two power-law regimes. This was noted in earlier work by Herman (2010), who wrote in reference to an earlier paper by Toyota: "However, contrary to how the above authors interpret their results, in both cases the change in slope of the FSD seems rather gradual than abrupt. Instead of a combination of two power laws glued together at a highly arbitrarily chosen floe diameter, another type of distribution would be desirable. It should reflect the observed gradually increasing deviation from a power-law distribution for decreasing floe diameter." Herman, A. (2010), Sea ice floe size distribution in the context of spontaneous scaling emergence in stochastic systems, Physical Review E, 81, DOI: 10.1103/ PhysRevE.81.066123 Furthermore, other researchers have found power-law behavior for the Antarctic FSD in which the exponent changes as the ice edge is approached, but without a critical floe size separating two power-law regimes (Paget et al, 2001; Lu et al, 2008). Returning to the current paper, a much simpler assumption for the FSD would have been a simple power law with one exponent. This would have eliminated the need for four parameters: D_cr, q, gamma_1, and P0. It would be interesting to know whether the results hold up under this simpler (and possibly more realistic) FSD. However, I would not insist that the authors re-do all their calculations, unless it's a simple thing to do (maybe just set D_cr

= D_mn and P0 = 0). But they should acknowledge that their results rest on the questionable split power-law formulation of the FSD.

We added an acknowledgement that other FSD's have been postulated for the transition from small–large floe sizes.

In a preliminary version of the model, we used a fixed breakup diameter $D_{\mathrm{bk}} = 30\,\mathrm{m}$ (based on anecdotal observations from our colleagues), and later found that the move to a breakup diameter based on an FSD and the local wavelength produced only small quantitative changes in our results. Therefore, we predict that adjusting the fine details of the in-cell FSD will not significantly impact our findings.

Page 3, equation (5). In the definition of P0, there is an exponent gamma_1. Is this the same gamma_1 as in equation (4b)? Why should it be the same exponent as in the probability density function? I don't understand the reasoning or the math for the use of gamma_1 here.

We have corrected $\gamma_0 \to \gamma_1$ and $\gamma_1 \to \gamma_2$ in the paragraph below Eqs. (4a–b).

We set the parameter $\mathbb{P}_0$ so that the proportion q of the floes have diameters greater than the predicted predicted breakup diameter, i.e.

$$\begin{aligned} 1 - q &= \int_{D_{\mathrm{mn}}}^{D_{\mathrm{pr}}} p(d)\ \mathrm{d}d \\ &= \mathbb{P}_0 + (1-\mathbb{P}_0)(1 - D_{\mathrm{cr}}^{\gamma_1}/D_{\mathrm{pr}}^{\gamma_1}) \\ \Rightarrow \quad \mathbb{P}_0 &= 1 - q\left(\frac{D_{\mathrm{pr}}}{D_{\mathrm{cr}}}\right)^{\gamma_1}, \end{aligned}$$

as given in the text. **We made no changes in response to this part of the comment.**

Page 4, equation (7) and following. What are the units of r_lat and w_lat? What is the value of the time step delta_t?

We added units for w_{lat} and clarified that r_{lat} is a fraction.

In the first paragraph of § 2, **we now explicitly give the time step in terms of the notation Δt.**

Page 6, lines 8-9, and Figure 2 (left panel). The text and the figure indicate that LESS attenuation of waves results in HIGHER mean ice concentration. I would have thought that less attenuation would allow more wave energy to penetrate into the ice pack and break up the ice, resulting in lower ice concentration. Please explain why less attenuation leads to higher ice concentration, and more attenuation leads to lower ice concentration.

We corrected the mistake in the text...

Page 6, line 15. "reducing the attenuation rate increases the impact..." I agree that reducing the attenuation rate SHOULD increase the impact of the waves, but Figure 2 shows that reducing the attenuation rate actually reduces the impact of the waves. The symbols for reduced attenuation rate (upward-pointing triangles) are much closer to the no-break-up case (crosses) than the symbols for increased attenuation rate (downward-pointing triangles). This doesn?t *make sense to me.*

. . . and the corresponding mistake in the Fig. 2 caption.

Page 7, line 8. "volume losses of 0.5 km^3 per grid cell" — This doesn't mean anything unless we know how big a grid cell is. On page 2, lines 15-16, we are told that the nominal resolution of the grid is 1 degree in latitude and 1 degree in longitude. The extent of 1 degree of longitude depends on latitude, so the size of a grid cell (in km^2) depends on latitude. At the latitude of the Antarctic Circle, 1 degree of longitude is about 44 km. So I calculate that the area of a grid cell is roughly 111 x 44 = 4884 km^2. A volume of 0.5 km^3 of ice spread over such a grid cell is about 10 cm of ice thickness (at 100% concentration) or 20 cm of ice thickness (at 50% concentration). So now I can understand roughly what a volume loss of 0.5 km^3 per grid cell means. Please help out the reader by providing this kind of information.

We now present volume losses per unit area.

Page 7, lines 20-23. If I understand this correctly, the eastern sector contains mostly first-year ice ("new ice"), with no memory of break-up, while the western sector presumably contains some multiyear ice, which retains memory of break-up?

We have rewritten this passage to clarify that summer volume losses are carried forward into winter in the western sector only, removing the word 'memory' that may cause confusion.

Technical Comments

Page 1, Abstract, line 2. "Model output shows that WAVE-INDUCED breakup..."

Added.

Page 2, equation (1). Cite Thorndike et al (1975), The Thickness Distribution of Sea Ice, JGR.

Citation added.

Page 3, line 18. "which is chosen to be equal TO the diameter..."

Typo corrected.

Page 3, line 20. Values are given for gamma_1 and gamma_2, but they should probably be gamma_0 and gamma_1. There is no gamma_2 in the equations.

Corrected: see earlier response.

Page 3, line 25. propagating through a uniform floe FIELD (?)

The predicted breakup diameter is calculated as the distance between successive peaks in strain produced by a regular wave propagating along a uniform ice cover of infinite extent.

We added the description "infinitely long" to the text.

Page 3, equation (6). Inside the integral, "pD" should be "p(D)" i.e. put parentheses around the "D"

Corrected $pD \longrightarrow p(d)d$.

Page 4, lines 21-22. In reference to Figure 1, in the left-hand panels showing wave height, it looks to me like the "sharp outer boundaries indicating the latitudes at which data is extracted from the wave model" are at the same latitude in each panel. But the next sentence says, "The boundary is farther north in winter..." I don?t see that the outer boundary of extracted data is farther north in the bottom panel. The outer circular boundary appears to be at exactly the same latitude in both panels. If the authors are referring to an INNER boundary that is several grid cells inside the outer boundary, they should mark it more clearly.

We added text to clarify that the "sharp out boundaries" we refer to are of non-zero wave heights.

Page 4, line 32. This sentence should refer to the middle column of Figure 1, just as the previous sentence refers to the left-hand column. Otherwise the reader may not shift her/his attention to the middle column.

We have amended this sentence.

Page 5, Figure 1, upper right panel showing concentration change. This panel is a bit too small — it's hard to see the regions of large change. A figure the size of Fig 3 would be better.

We changed to orientation of the array to maximise the size of the panels.

Page 7, line 9. "bottom-left panel" should be "bottom-right panel"

Typo corrected.

Page 7, line 17. "ice volume per latitude" should be "ice volume per degree of latitude". Similarly in Figure 3 (in the title of the bottom right panel) and in the caption.

Changes made.

Page 8, Figure 3. The eastern and western sectors should be marked in the upper panels (the maps).

Sectors are now marked.

Page 9, lines 2-3. "If the community judges the impacts..." ? maybe better to say "If further research finds the impacts..."

We made the suggested change.

Page 11. "Schwinger" should be "Schweiger"

Typo corrected.